

# Isothermal Crystallization of Metallocene-Based Polypropylenes with Different Isotacticity and Regioregularity

Jun-Ting Xu, Fang-Xiao Guan, Tariq Yasin, Zhi-Qiang Fan

Department of Polymer Science & Engineering, Zhejiang University, Hangzhou 310027, People's Republic of China

Received 28 November 2002; accepted 8 April 2003

**ABSTRACT:** Three polypropylenes with various isotacticities and regioregularities were prepared with metallocene catalysts at different polymerization temperatures. WAXD results showed that the relative content of  $\gamma$  crystals in polypropylenes increased as isotacticity decreased. It was found that the  $\gamma$  crystal overcame the  $\alpha$  crystal and became predominant in polypropylene of low isotacticity and high regioerrors. More  $\gamma$  crystals were also formed at higher crystallization temperatures. The isothermal crystallization kinetics of  $\alpha$  and  $\gamma$  crystals were compared and the metastability of these two crystal phases was interpreted in terms of the crystallization kinetics. It was observed that the  $\alpha$  crystal has a faster crystallization rate than that of the  $\gamma$  crystal and, thus, higher stability at low temperature. By contrast, the  $\gamma$  crystal tends to have a faster crystallization

rate and becomes more stable at high temperature. The metallocene-based polypropylenes with different isotacticities have similar Avrami exponents. As the content of the  $\gamma$  crystal increases, double melting peaks become more evident. Equilibrium melting temperatures were derived from Hoffman–Weeks analysis and very close equilibrium melting temperatures were obtained, 185.5 and 184.0°C, for two metallocene-based polypropylenes containing major  $\alpha$  crystals and one of 182.5°C for the polypropylene with predominant  $\gamma$  crystals. © 2003 Wiley Periodicals, Inc. *J Appl Polym Sci* 90: 3215–3221, 2003

**Key words:** isotactic polypropylene; metallocene; isotacticity; isothermal crystallization; equilibrium melting temperature

## INTRODUCTION

There are usually three crystal forms in isotactic polypropylene. The most commonly observed is the monoclinic  $\alpha$  form.<sup>1</sup> The second is the hexagonal  $\beta$  form, which is obtained by addition of a nucleation agent or under stress and can transform into the  $\alpha$  form upon heating. The third one, the  $\gamma$  crystal form, was first identified as triclinic but recently was determined to be orthorhombic.<sup>2</sup> For the highly isotactic polypropylenes prepared by conventional Ziegler–Natta catalysts, the  $\gamma$  crystal form is formed only at high pressure<sup>3,4</sup> or in low molecular weight homopolymers<sup>25,6</sup> or in propylene copolymers.<sup>7,8</sup> Therefore, it is difficult to compare the crystallization behavior of  $\alpha$  and  $\gamma$  crystals at the same crystallization conditions. By using metallocene catalysts, the isotacticity and regioregularities of isotactic polypropylene can be easily controlled by selecting suitable catalysts and polymerization conditions,<sup>9,10</sup> and, thus,  $\gamma$  crys-

tals are also formed under common crystallization conditions in metallocene-based isotactic polypropylenes.<sup>11,12</sup> Since formations of  $\alpha$  and  $\gamma$  crystals are competitive under the same crystallization condition, crystallization kinetics is very important. The metastability of  $\alpha$  and  $\gamma$  crystals is still controversial, but most of the discussion has been concentrated on thermodynamics. Keller and Cheng pointed out that the metastable phase with higher stability also possesses a faster rate of formation.<sup>13</sup> As a result, studies on crystallization kinetics can help us understand the metastability of  $\alpha$  and  $\gamma$  crystals from the viewpoint of kinetics. However, to our knowledge, there are no reports yet on the crystallization kinetics of  $\alpha$  and  $\gamma$  crystals under the same conditions.

In this article, three polypropylenes with various isotacticities and regioregularities were prepared with metallocene catalysts at different polymerization temperatures. In two of these isotactic polypropylenes,  $\alpha$  crystals are predominantly formed, but the other one contains mainly  $\gamma$  crystals. The isothermal crystallization behaviors of  $\alpha$  and  $\gamma$  crystals were investigated and compared.

## EXPERIMENTAL

### Materials

Polypropylene samples with various isotacticities and regioregularities were prepared by propylene poly-

Correspondence to: Z.-Q. Fan (fanzq@zju.edu.cn).

Contract grant sponsor: National Natural Science Foundation of China; contract grant numbers: 29734144; 59703002.

Contract grant sponsor: Special Funds for Major State Basic Research Projects; contract grant number: G1999064803.

**TABLE I**  
Structural Characteristics of the Polypropylene Samples

Samples	$T_p^a$ (°C)	[ <i>mmmm</i> ] (%)	$M_n$	2,1 m-in <sup>b</sup> (%)	1,3-in <sup>c</sup> (%)	Total regioerrors <sup>d</sup> (%)
mPP1	30	80	63,300	0.37	0.00	0.37
mPP2	50	91	20,200	0.42	0.16	0.58
mPP3	70	71	12,800	0.10	0.52	0.62

<sup>a</sup> Temperature of polymerization.

<sup>b</sup> Percentage of 2,1-insertion (meso form) in the polymer chain measured by <sup>13</sup>C-NMR.

<sup>c</sup> Percentage of 1,3-insertion in the polymer chain measured by <sup>13</sup>C-NMR.

<sup>d</sup> Sum of the 2,1-insertion and the 1,3-insertion percentages.

merization at different temperatures employing *rac*-(CH<sub>3</sub>)<sub>2</sub>Si[(2,4,6-CH<sub>3</sub>)<sub>3</sub>Ind]<sub>2</sub>ZrCl<sub>2</sub> as a catalyst and methylaluminoxane (MAO) as a cocatalyst. Details of the polymerization were described elsewhere.<sup>14</sup> The isotacticity of the polypropylenes was determined using NMR, which was carried out on a Bruker DMX 500 spectrometer at 100°C with *o*-C<sub>6</sub>D<sub>4</sub>Cl<sub>2</sub> as a solvent. The concentration of the polymer was 20% w/v, the delay time was 10 s, and scanning times were 3000. The viscosity-average molecular weight of the polymers were measured by viscometry with an Ubbelohde-type viscometer using decahydronaphthalene as a solvent at 135 ± 0.1°C. The concentration of the solution was ~0.1 % g/mL and a small amount of an antioxidant (4,6-di-*t*-butyl-*p*-cresol) was added to the solution. The viscosity-average molecular weight was calculated according to the relationship<sup>15</sup>  $[\eta] = KM_v^\alpha$  ( $K = 1.10 \times 10^{-4}$ ,  $\alpha = 0.80$ ). Some structural characteristics of the polymers are given in Table I.

### DSC experiments

Isothermal crystallization kinetics of the polypropylenes was carried out on a Perkin-Elmer Pyris-1 calorimeter. About 2–3 mg of the samples was sealed with aluminum pans and heated to 200°C, held for 5 min, and then cooled at a rate of 100°C/min to the crystallization temperatures and held until crystallization was completed. The change of heat flow with time was recorded upon crystallization. After isothermal crystallization was completed, the samples were heated to 180°C immediately from the crystallization temperature at a rate of 10°C/min.

### Wide-angle X-ray diffraction (WAXD)

X-ray diffraction experiments were performed on a Rinter 2500 X-ray diffractometer (40 kV, 300 mA) using Ni-filtered CuK $\alpha$  radiation in 0.02° steps from 5° to 45°. The samples were quenched with ice water after isothermal crystallization at different temperatures

and then WAXD experiments were carried out immediately.

## RESULTS AND DISCUSSION

### WAXD result

Figure 1 shows WAXD graphs of three metallocene-based polypropylenes with different isotacticities crystallized at both higher and lower temperatures. One can see both the characteristic reflections of the  $\alpha$  crystal phase at  $2\theta = 18.6^\circ$  and the  $\gamma$  crystal phase at  $2\theta = 20.05^\circ$ . The percentage of  $\gamma$  crystals increases with decreasing isotacticity and regioregularity. In mPP1, the  $\alpha$  crystal is dominant, and the content of the  $\gamma$  phase was very close to that of the  $\alpha$  phase in mPP2 at a higher crystallization temperature, but the  $\gamma$  phase becomes the major component in mPP3. This is because the polypropylenes with lower isotacticity contain more short crystallizable propylene sequences, which are favorable to the formation of the  $\gamma$  crystal phase. Additionally, regioerrors caused by 1,3-insertion further interrupt the isotactic polypropylene sequence; thus, the  $\gamma$  phase becomes dominant when the sample contains more of a 1,3-insertion structure. It

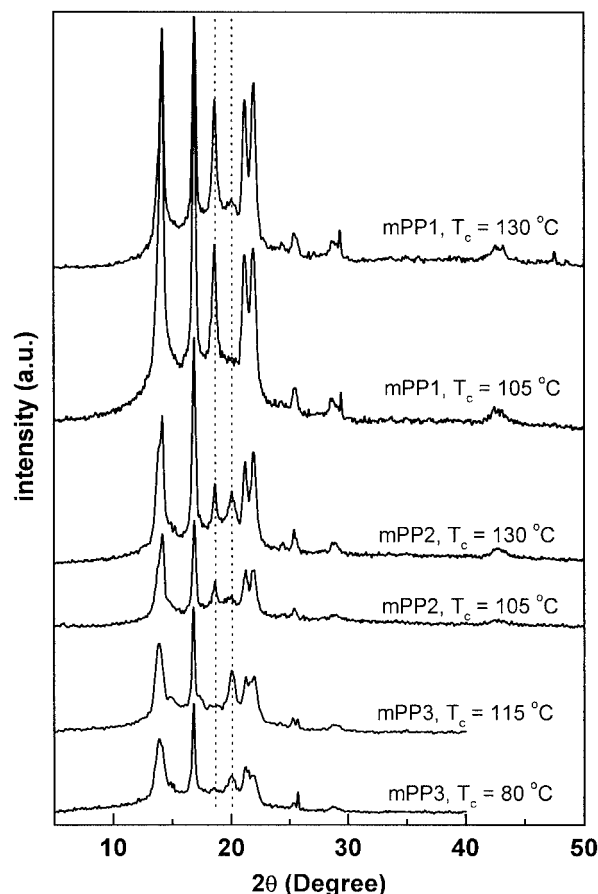


**Figure 1** WAXD graphs of mPP1, mPP2, and mPP3 crystallized at different temperatures.

was also observed that the content of the  $\gamma$  crystal phase is larger at a higher crystallization temperature. Alamo et al. revealed that the content of the  $\gamma$  crystal phase increases with the crystallization temperature and then undergoes a maximum with respect to the crystallization temperature.<sup>16</sup> In Figure 1, we can see that the positions of the characteristic reflections for the  $\alpha$  and  $\gamma$  crystal phases remain the same, even though these polypropylene samples have different isotacticities and crystallize at different temperatures, indicating that isotacticity does not affect the dimension of the unit cell of the crystals.

**Isothermal crystallization kinetics**

The isothermal crystallization kinetics of the polypropylenes can be interpreted in terms of the Avrami equation<sup>17</sup>:

$$1 - X(t) = \frac{\Delta H_{t=\infty}^c - \Delta H_t^c}{\Delta H_{t=\infty}^c - \Delta H_{t=0}^c} = \exp(-kt^n) \quad (1)$$

where  $X(t)$  is the relative crystallinity at time  $t$  and  $\Delta H_{t=\infty}^c$  and  $\Delta H_t^c$  are the crystallization enthalpies on complete crystallization and after time  $t$ , respectively. Therefore, we have

$$\ln\{-\ln[1 - X(t)]\} = \ln k + n \ln t \quad (2)$$

The crystallization rate constant  $k$  and the Avrami exponent  $n$  can be determined from the intercept and slope in the plot of  $\ln\{-\ln[1 - X(t)]\}$  versus  $\ln(t)$ , respectively. The crystallization half-time  $t_{1/2}$  is related to the crystallization rate constant by the following equation:

$$\ln(t_{1/2}) = [\ln(\ln 2) - \ln k]/n \quad (3)$$

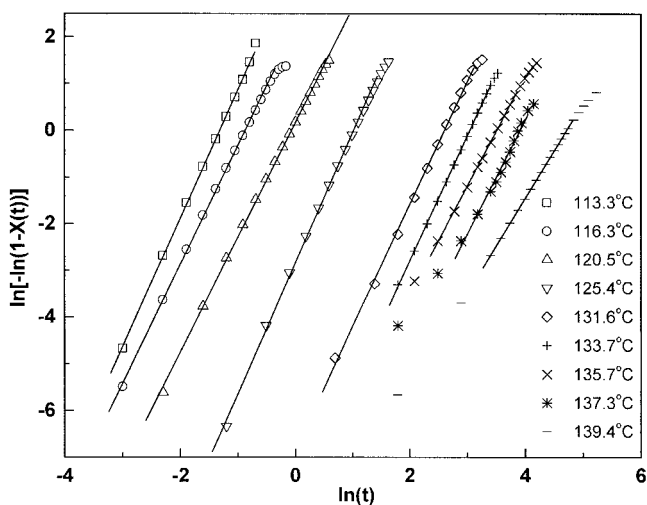


**Figure 2** Avrami plots of mPP1 crystallized at different temperatures.

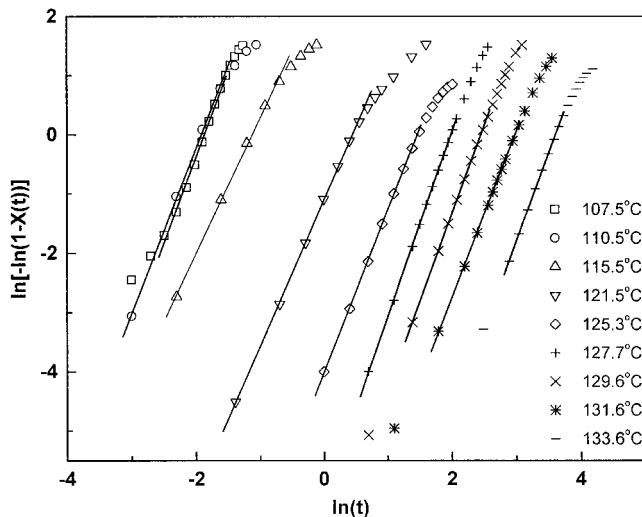


**Figure 3** Avrami plots of mPP2 crystallized at different temperatures.

The Avrami plots for mPP1, mPP2, and mPP3 are shown in Figures 2–4 and the data are summarized in Table II. It was found that the Avrami exponents of these three polypropylene samples with different isotacticities are basically between 2.0 and 3.0 and they show no large difference. This indicates that all these three metallocene-based polypropylenes can form less perfect spherulite morphology. The polarized light microscope graphs of these three polymers crystallized from the xylene solution confirm the ability of forming spherulites of mPP1, mPP2, and mPP3. Perfect spherulite morphology with Maltese crosses was observed for all polymers (not shown here). The spherulite morphology becomes less perfect for PP crystallized from the melt, leading to an Avrami exponent smaller than 3.0. When the logarithmic crys-

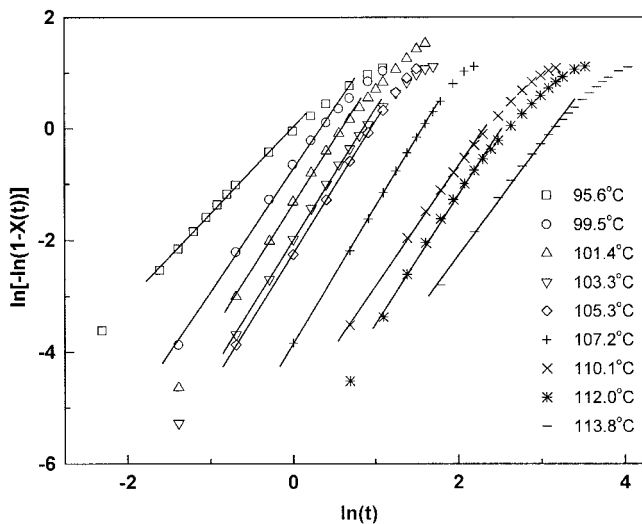


**Figure 4** Avrami plots of mPP3 crystallized at different temperatures.

TABLE II  
Parameters for Isothermal Crystallization Kinetics

Samples	$T_c$ (°C)	$T_m$ (°C)	$\ln k$	$n$	$\ln t_{1/2}$ (min)
mPP1	113.3	151.9	3.62	2.8	-1.45
	116.3	152.4	2.23	2.6	-1.02
	120.5	153.6	0.16	2.5	-0.21
	125.4	155.4	-2.84	2.8	0.89
	131.6	155.8	-6.83	2.6	2.47
	133.7	156.6	-8.14	2.7	2.90
	135.7	158.0	-8.22	2.4	3.34
	137.3	158.6	-9.54	2.4	3.76
	139.4	160.0	-9.64	2.1	4.52
	mPP2	107.5	145.1	5.39	2.9
110.5		145.3	5.32	2.8	-2.04
115.5		146.1	2.55	2.3	-1.28
121.5		147.8	-1.12	2.5	0.31
125.3		149.1	-4.02	2.7	1.33
127.7		151.0	-6.17	3.1	1.87
129.7		151.6	-7.27	3.0	2.30
131.6		152.7	-8.36	2.8	2.85
133.6		153.9	-10.68	3.0	3.48
mPP3		95.6	123.0	0.014	1.6
	99.5	125.4	-0.74	2.2	0.17
	101.4	126.9	-1.37	2.3	0.44
	103.3	128.0	-2.01	2.4	0.70
	105.3	129.6	-2.24	2.4	0.79
	107.2	130.7	-3.85	2.5	1.42
	110.1	132.9	-4.97	2.2	2.15
	112.0	133.9	-5.80	2.3	2.37
	113.8	135.1	-6.27	2.0	2.95

tallization rate constant,  $\ln k$ , is plotted versus  $1/T$ , the activation energy of crystallization is obtained from the slope.

As shown in Figure 5, one can see that mPP1 and mPP2 have similar crystallization activation energies,

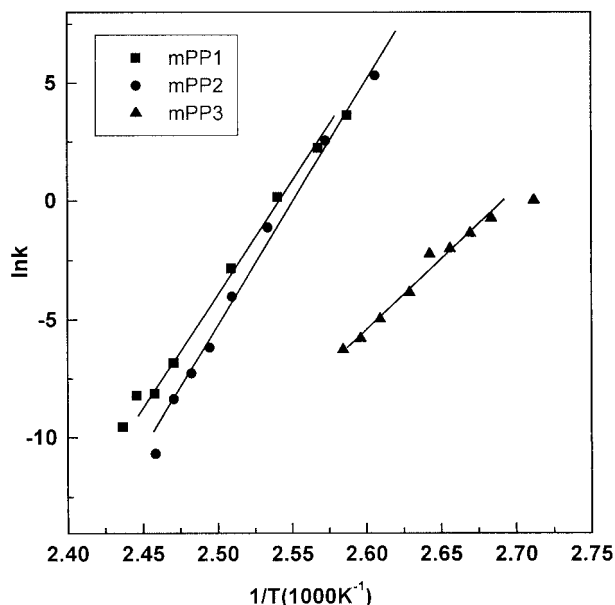


Figure 5 Plots of  $\ln k$  versus  $1/T$  for mPP1, mPP2, and mPP3.

but the slope of mPP3 is evidently lower than those of mPP1 and mPP2, indicating the smaller crystallization activation energy of mPP3. A possible reason is that the  $\gamma$  crystal phase becomes dominant in mPP3 and the activation energy for the formation of the  $\gamma$  crystal phase is smaller. The most important effect shown by Figure 5 is the change of the crystallization rates of  $\alpha$  and  $\gamma$  crystals with the temperature. One can see that  $\alpha$  crystals have a faster crystallization rate than that of the  $\gamma$  crystals at the crystallization temperatures employed in the present study. However, when the crystallization temperature is extrapolated to higher temperature,  $\gamma$  crystals tend to crystallize faster than  $\alpha$  crystals. The inversion temperature is about 152°C. Based on the metastability theory proposed by Keller and Cheng that faster crystallization and higher stability of the metastable phase are interlinked,<sup>13</sup> we can clearly draw the conclusion that the  $\gamma$  crystal is more stable than the  $\alpha$  crystal at high temperature, but it becomes metastable at low temperature. This is the reason why the relative content of the  $\gamma$  crystal increases as the crystallization temperature increases. As a result, the metastability of the  $\alpha$  and  $\gamma$  crystals in polypropylene can be perfectly explained from the viewpoint of crystallization kinetics. Such an explanation is also in accordance with the conclusion drawn from the viewpoint of thermodynamics.<sup>18,19</sup>

In examining the variation of the crystallization half-time ( $t_{1/2}$ ) with the crystallization temperature (Fig. 6), we find that mPP3 has a smaller slope than those of mPP1 and mPP2, confirming that the crystallization rate of mPP1 and mPP2 has a stronger dependence on the crystallization temperature.

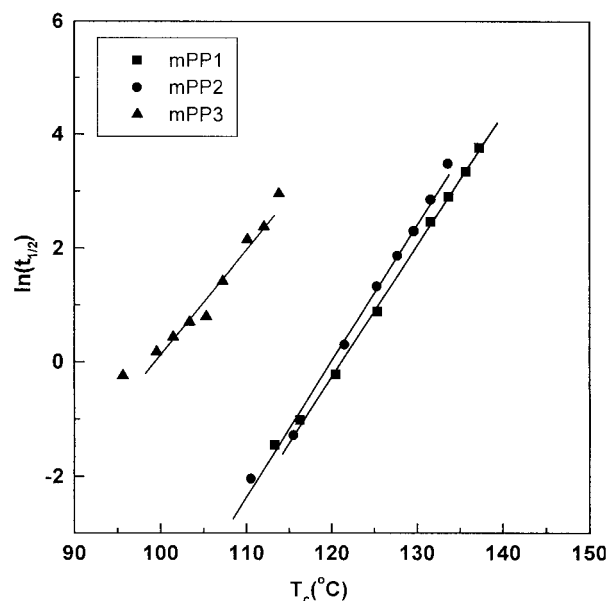
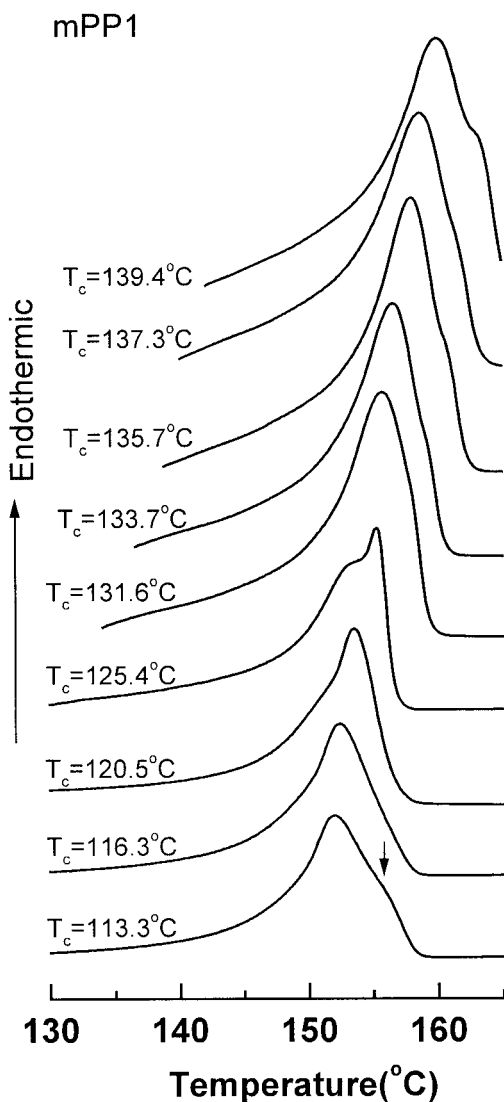


Figure 6 Crystallization half-time of mPP1, mPP2, and mPP3 at different crystallization temperatures.



**Figure 7** DSC melting curves of mPP1 after crystallization at different crystallization temperatures. The arrows indicate the shoulder melting peaks.

#### Subsequent melting behavior

Figures 7–9 show the melting DSC curves after crystallization at various temperatures. Comparing these melting traces, two phenomena are noticed: First, a small melting peak can be found at higher temperature than that of the major melting peaks when polypropylenes crystallize at lower temperatures, for example, mPP1 at  $T_c = 113.3^\circ\text{C}$ , mPP2 at  $T_c = 107.5$ ,  $110.5$ , and  $115.5^\circ\text{C}$ , and mPP3 at  $T_c = 95.6$ ,  $99.5$ , and  $101.4^\circ\text{C}$ . These higher-temperature peaks are produced by melting–recrystallization–melting during the melting process, since less-ordered crystals are formed at lower crystallization temperatures due to larger supercooling and the formation of the higher-temperature melting peaks can be suppressed at a higher heating rate (not shown here).<sup>20</sup> Such melting–recrystallization–melting behavior becomes clearer

when the polymerization temperature of the sample increases, which leads to less-ordered polymer chains. Second, an overlapping melting peak, as indicated by arrows in Figures 8 and 9, also appears in mPP2 and mPP3 at lower temperature than that of the major melting peak, but such a peak is not evident in mPP1. Both the melting temperatures of the major peak and the shoulder peak increase with the crystallization temperature. These two melting peaks may be produced by  $\alpha$  and  $\gamma$  crystals, respectively. However, it should be noted that the major melting peak in mPP3 should be assigned to the  $\gamma$  crystal phase and the smaller peak at lower temperature is attributed to the  $\alpha$  crystal phase, since the  $\gamma$  crystal phase is the predominant crystalline component in this sample, while the major melting peak is produced by the  $\alpha$  crystal phase in mPP1 and mPP2.

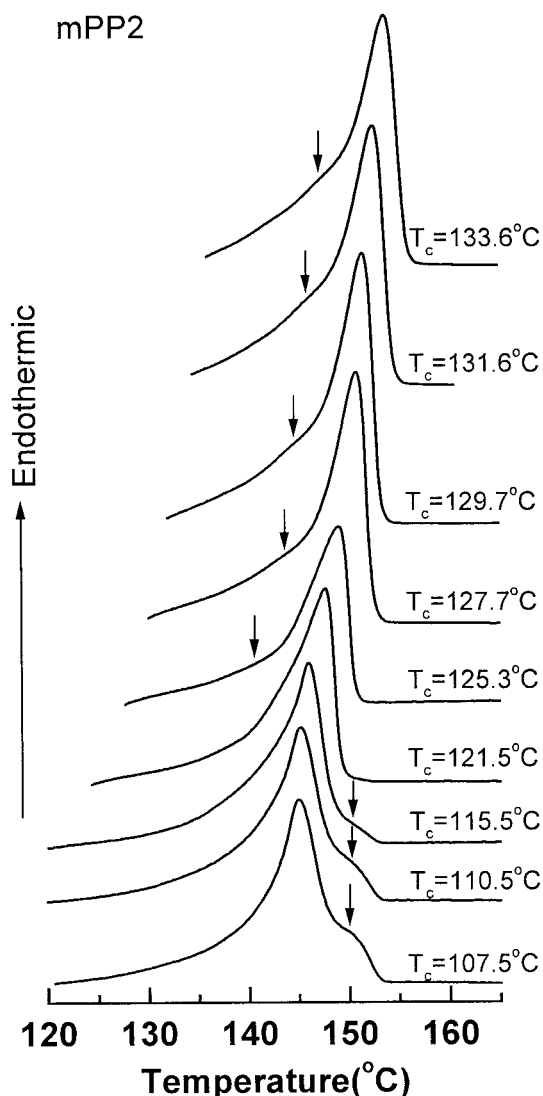


**Figure 8** DSC melting curves of mPP2 after crystallization at different crystallization temperatures. The arrows indicate the shoulder melting peaks.

### Equilibrium melting temperature

The equilibrium melting temperature ( $T_m^0$ ) of the polymers can be obtained by extrapolating the plot of the melting temperature ( $T_m$ ) versus the crystallization temperature ( $T_c$ ) to  $T_c = T_m = T_m^0$  in terms of the Hoffman-Weeks equation<sup>21</sup>:

$$T_m = (1 - 1/\gamma)T_m^0 + T_c/\gamma \quad (4)$$

where  $\gamma$  is the ratio of the crystal thickness to the thickness of the initial nucleus at the crystallization temperature  $T_c$ .

Such an extrapolation is shown in Figure 10. It is found that these three metallocene-based polypropylenes have very close equilibrium melting temperatures, which are 185.5, 184.0, and 182.5°C for mPP1, mPP2, and mPP3, respectively. Therefore, two conclu-

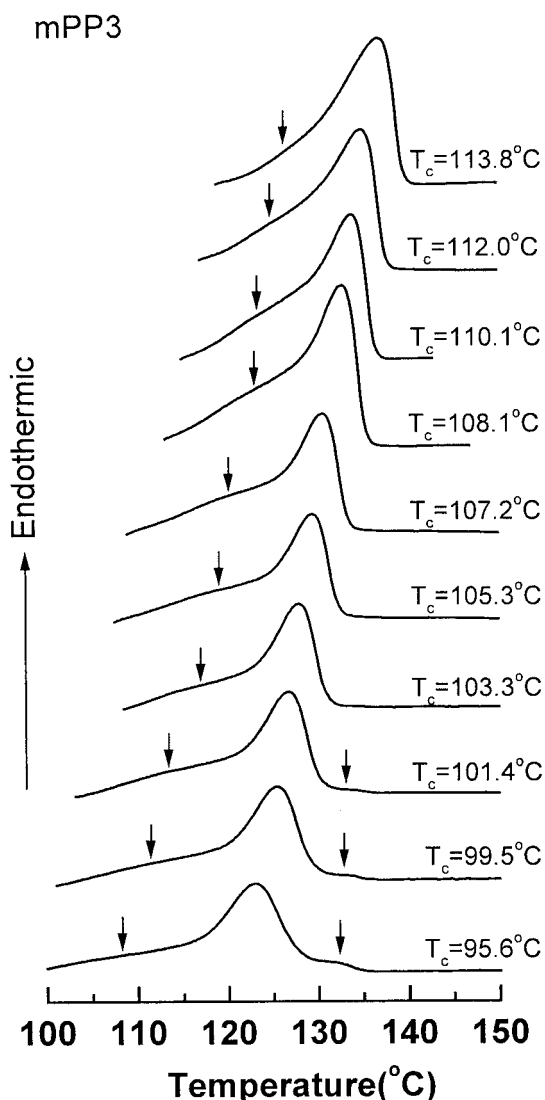


**Figure 9** DSC melting curves of mPP3 after crystallization at different crystallization temperatures. The arrows indicate the shoulder melting peaks.

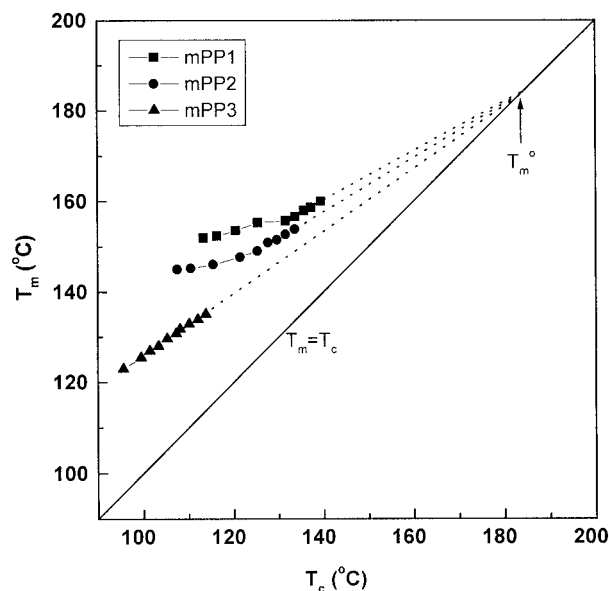


**Figure 10** Hoffman-Weeks extrapolation for the equilibrium melting temperatures of mPP1, mPP2, and mPP3.

sions can be drawn from this finding: First, the equilibrium melting temperature of the  $\gamma$  crystal is very close to that of  $\alpha$  crystal, since the mPP3 contains mainly  $\gamma$  crystals but  $\alpha$  crystals are predominant in mPP1 and mPP2. However, considering the effect of stereo- and regioirregularities on the melting temperature, the equilibrium melting temperature of the  $\gamma$  crystal may be slightly larger than that of the  $\alpha$  crystal containing the same isotacticity, as expected by other authors.<sup>2</sup> Second, the equilibrium melting temperature of the  $\alpha$  crystals in mPP1 and mPP2 is not seriously lowered by stereo- and regioirregularities. This shows that stereo- and regioirregularities can be included in the crystal lattice. The equilibrium melting temperatures of these three metallocene-based polypropylenes are very close to the value widely reported for conventional polypropylene: 186°C.<sup>22</sup> Bonds and Spruiell also found that two metallocene-based polypropylenes had similar equilibrium melting temperatures of about  $186 \pm 2^\circ\text{C}$  and the equilibrium melting temperature of the  $\gamma$  crystal is  $178 \pm 4^\circ\text{C}$ .<sup>23</sup> However, Janimak reported that the equilibrium melting temperature changes from 436.6 to 457.4 K when the isotacticity increases from 0.787 to 0.988 for some conventional polypropylenes.<sup>24</sup>

### CONCLUSIONS

WAXD results showed that the metallocene-based polypropylenes (mPP1 and mPP2) with higher isotacticity and regioirregularity contain mainly  $\alpha$  crystals, whereas  $\gamma$  crystals are predominant in mPP3 of lower isotacticity and regioirregularity. All these three metallocene-based polypropylenes have similar Avrami exponents in spite of different isotacticities. It was found

that the  $\gamma$  crystal-predominant mPP3 has a smaller crystallization rate constant at low temperature, indicating that it has lower stability than that of the  $\alpha$  crystal. By contrast, the  $\gamma$  crystal tends to crystallize faster and shows higher stability at high temperature. As the content of the  $\gamma$  crystal increases, double melting peaks become more evident. The two metallocene-based polypropylenes containing major  $\alpha$  crystals and the one with predominant  $\gamma$  crystals have very close equilibrium melting temperatures.

Support by the National Natural Science Foundation of China (Grant Nos. 29734144 and 59703002) and the Special Funds for Major State Basic Research Projects (Grant No. G1999064803) are gratefully acknowledged by the authors.

## References

1. Bruckner, S.; Meille, S. V.; Petraccone, V.; Pirozzi, B. *Prog Polym Sci* 1991, 16, 361.
2. Bruckner, S.; Meille, S. V. *Nature* 1989, 340, 455.
3. Campbell, R. A.; Phillips, P. J.; Lin, J. S. *Polymer* 1993, 34, 4809.
4. Mezghani, K.; Phillips, P. J. *Polymer* 1997, 38, 5725.
5. Morrow, D. R.; Newman, B. A. *J Appl Phys* 1968, 39, 4944.
6. Lotz, B.; Graff, S.; Wittmann, J. C. *J Polym Sci Part B Polym Phys* 1986, 24, 2017.
7. Turner-Jones, A. *Polymer* 1971, 12, 487.
8. Mezghani, K.; Phillips, P. J. *Polymer* 1995, 36, 2407.
9. Rieger, B.; Mu, X.; Mallin, D. T.; Rausch, M. D.; Chien, J. C. W. *Macromolecules* 1990, 23, 3559.
10. Perez, E.; Zucchi, D.; Sacchi, M. C.; Forlini, F.; Bello, A. *Polymer* 1999, 40, 675.
11. Fischer, D.; Mulhaupt, R. *Macromol Chem Phys* 1994, 195, 1433.
12. Thomann, R.; Wang, C.; Kressler, J.; Mulhaupt, R. *Macromolecules* 1996, 29, 8425.
13. Keller, A.; Cheng, S. Z. D. *Polymer* 1998, 39, 4461.
14. Fan, Z. Q.; Yasin, T.; Feng, L. X. *J Polym Sci Part A Polym Chem* 2000, 38, 4299.
15. Kinsinger, J. B.; Hugres, R. E. *J Phys Chem* 1959, 63, 2001.
16. Alamo, R. G.; Kim, M. H.; Galante, M. J.; Isasi, J. R.; Melkern, L. *Macromolecules* 1999, 32, 4050.
17. Avrami, M. *J Chem Phys* 1939, 7, 1103.
18. Mezghani, K.; Phillips, P. J. *Polymer* 1998, 39, 3735.
19. Foresta, T.; Piccarolo, S.; Goldbeck-Wood, G. *Polymer* 2001, 42, 1167.
20. Celli, A.; Fichera, A.; Marega, C.; Marigo, A.; Paganetto, G.; Zannetti, R. *Eur Polym J* 1993, 29, 1037.
21. Hoffman, J. D.; Weeks, J. J. *J Res Natl Bur Stand* 1962, 66, 13.
22. *Polymer Data Handbook*; Mark, J. E., Ed.; Oxford University: Oxford, 1999.
23. Bond, E. B.; Spruiell, J. E. *J Appl Polym Sci* 2001, 81, 229.
24. Cheng, S. Z. D.; Janimak, J. J.; Zhang, A. Q.; Hsieh, E. T. *Polymer* 1991, 32, 648.